Increased Hyaluronan Synthase-2 mRNA Expression and Hyaluronan Accumulation with Choroidal Thickening: Response during Recovery from Induced Myopia

Jody A. Summers Rada,[1,2] *Allan F. Wiechmann,*[1,2,3] *Lindsey R. Hollaway,*[1] *Bruce A. Baggenstoss,*[4] *and Paul H. Weigel*[4]

Purpose. Several studies have convincingly shown that in chicks, compensation for imposed focus involves immediate changes in choroid thickness. The molecular events associated with choroidal thickening and the regulation of the choroidal response are largely unknown.

Methods. Form-deprivation myopia was induced in the right eyes of 2-day-old chicks by the application of translucent occluders for 10 days and was followed by unrestricted vision for an additional 1 to 20 days (recovery). Individual choroids were isolated from treated and control eyes and used for reverse transcription–quantitative PCR, hyaluronan (HA) localization with biotinylated hyaluronic acid binding protein (b-HABP), and analyses of HA size and concentration by size exclusion chromatography-multiangle laser light scattering (SEC-MALLS).

Results. *HAS2* gene expression increased significantly after 6 hours of unrestricted vision (>7-fold) and peaked at 24 hours (>9-fold). In untreated eyes, HA was localized to perivascular sheaths of larger choroidal blood vessels; however, after 4 to 15 days of recovery, intense labeling for HA was detected throughout the thickened choroidal stroma. Analyses of choroidal HA by SEC-MALLS indicated that HA concentration was significantly increased in recovering choroids compared with controls after 4 to 8 days of recovery (≈3.5-fold).

Conclusions. Newly synthesized HA accumulates in the choroidal stroma of recovering eyes and is most likely responsible for the stromal swelling observed during recovery from myopia. This HA accumulation is initiated by a rapid increase in choroidal expression of the *HAS2* gene in response to myopic defocus. (*Invest Ophthalmol Vis Sci.* 2010;51:6172–6179) DOI:10.1167/iovs.10-5522

Clinical and experimental studies have shown convincingly that refractive development occurs under both genetic and environmental influences. Deprivation of form vision, either through ocular pathology in humans[1–4] or from the application of translucent occluders in animal models,[5] results in axial elongation and myopia. Moreover, the imposing of hyperopic defocus on the retina with minus lenses[6,7] causes an accelerated rate of axial elongation and negative refractive error compared with the contralateral untreated eye. These visually induced changes in ocular size and refraction are reversible; restoration of unrestricted vision (and the resultant myopic defocus) results in a temporary cessation of axial growth, eventually leading to the reestablishment of emmetropia ("recovery") in the formerly deprived eye.[8] The response to defocus is rapid, leading to detectable changes in vitreous chamber depth within hours.[9] Although the retinal signals leading to recovery from form deprivation-induced myopia may be different from those that are generated during the induction of hyperopia with positive lenses, optical correction of form deprivation-induced myopia with negative lenses inhibits recovery, suggesting that recovery from form deprivation myopia is a result of an active emmetropization process to correct the imposed myopic defocus.[10]

Although the mechanisms underlying visually guided changes in ocular elongation have yet to be determined, it is widely accepted that local factors within the eye play an important role in the regulation of ocular growth because form deprivation myopia, recovery from induced myopia, and compensation for positive and negative lenses can occur in the absence of an intact optic nerve.[11] Because of its location between the retina and the sclera, the choroid is positioned to transmit growth signals directly to the sclera, where they can regulate scleral extracellular matrix remodeling and the rate of ocular elongation. Similar to the mammalian choroid, the chick choroid consists of a layer of choriocapillaries that are adjacent to Bruch's membrane and larger blood vessels nearer the sclera.[12,13] Additionally, the chick choroid contains numerous thin-walled, endothelial-lined vessels that exhibit structural features of lymphatic vessels (lymphatic lacunae).[12–15]

Studies by Wallman et al.[16] and Liang et al.[17] have shown that the chick choroid undergoes a rapid and dramatic increase in thickness in response to myopic defocus as a result of previous form deprivation or the application of positive lenses. As visualized by light and electron microscopy, the visually driven thickening of the chick choroid results, at least in part, from swelling of the choroidal lacunae[14,16] and from extravascular tissue edema.[15] Concomitant with choroidal thickening, the rate of vitreous chamber elongation slows dramatically,[18] as does proteoglycan synthesis in the chick sclera.[19] It is, therefore, hypothesized that the increase in choroidal thickness is a rapid mechanism for reducing refractive error by moving the retina to the focal point.[16] Similar changes in choroid thickness have been observed in tree shrews and primates, but to a lesser degree.[20–22]

Previous microarray analyses identified hyaluronan synthase 2 (*HAS2*) as a gene significantly upregulated in the choroids

From the Departments of [1]Cell Biology, [3]Ophthalmology, and [4]Biochemistry and Molecular Biology and the [2]Oklahoma Center of Neuroscience, University of Oklahoma Health Science Center, Oklahoma City, Oklahoma.

Supported by National Eye Institute Grant R01 EY09391 (JASR), OCAST Grant HR06-125 (AFW), and National Institute of General Medical Sciences Grant R01 GM35978 (PHW).

Submitted for publication March 14, 2010; revised April 21, May 14 and 24, and June 1, 2010; accepted June 3, 2010.

Disclosure: **J.A. Summers Rada**, None; **A.F. Wiechmann**, None; **L.R. Hollaway**, None; **B.A. Baggenstoss**, None; **P.H. Weigel**, None

Corresponding author: Jody Summers Rada, Department of Cell Biology, University of Oklahoma Health Science Center, BRC, Room 266, 975 NE 10th Street, Oklahoma City, OK 73104; jody-rada@ouhsc.edu.

after 24 hours of recovery (unpublished data, 2007). *HAS2* is a member of the class 1 HAS family and is 1 of 3 HAS isoenzymes encoded by distinct genes typically found in vertebrates. These enzymes are responsible for the synthesis of hyaluronan (HA), a nonsulfated glycosaminoglycan distributed widely throughout connective, epithelial, and neural tissues.[23,24] *HAS2* and *HAS3* genes are present in the *Gallus gallus* genome, but a *HAS1* gene is either absent or not yet annotated. In the present study, we show that HAS2 mRNA pools in isolated choroids increased rapidly (within 6 hours of myopic defocus), resulting in significant HA accumulation in the choroids of recovering eyes. The accumulation of HA within the choroidal stroma likely accounts for the rapid thickening of the choroid during compensation for myopic defocus.

Materials and Methods

Animals

White Leghorn cockerels (*G. gallus*) were obtained as 2-day-old hatchlings from Ideal Breeding Poultry Farms (Cameron, TX). Birds were housed in temperature-controlled brooders with a 12-hour light/12-hour dark cycle and were given food and water ad libitum. Form-deprivation myopia was induced in 2-day-old chicks by applying translucent plastic goggles as previously described.[19,25] Briefly, chicks were lightly anesthetized with isoflurane (Vedco Inc., St. Joseph, MO), and hemispheric goggles, cut from the bottoms of 15-mL round-bottom test tubes, were affixed to the feathers around the right eyes of 2-day-old chicks with cyanoacrylate adhesive. Goggles remained in place for 10 days, after which either chicks were killed for isolation of ocular tissues from control (contralateral untreated eyes) and form-deprived eyes or goggles were removed and chicks were allowed to experience unrestricted vision (recovery) for 0, 1, 4, 7, 8, and 15 days. The left eyes of all the chicks were never goggled and were used as controls. Chicks were checked twice daily for condition of occluders.

The treatment regimen used in this study was based on our previous studies, which demonstrate that restoration of unrestricted vision from previous form deprivation for 10 days results in significant changes in choroid thickness and permeability and significant decreases in glycosaminoglycan synthesis in the posterior sclera and in the rate of ocular elongation after only 1 day of recovery.[18,19] Based on these previous studies, the visual conditions selected for the present study were designed to identify molecules involved in the early phase of the choroidal response that may play a role in the regulation of ocular growth during recovery from induced myopia. Animals were maintained and used in accordance with the Animal Welfare Act and National Institutes of Health Guidelines and the ARVO Statement for the Use of Animals in Ophthalmic and Vision Research. All procedures were approved by the Institutional Animal Care and Use Committee of the University of Oklahoma Health Sciences Center.

Tissue Preparation

Chicks were euthanatized by an overdose of isoflurane inhalant anesthetic (Iso-Thesia; Vetus Animal Health, Rockville Center, NY), and eyes were enucleated. Each eye was divided into anterior and posterior hemispheres by making a circumferential cut around the equator, and the posterior hemisphere was gently cleaned of all vitreous, pectin, and muscle. One 5-mm tissue punch was excised from the posterior pole using a dermal biopsy punch (Miltex Instrument Company, Inc., Bethpage, NY) containing the sclera, choroid, retinal pigment epithelium (RPE), and retina. Some tissue punches were fixed in neutral-buffered formalin for paraffin embedding and tissue sectioning, and other punches were transferred to Petri plates containing 1 drop of 0.1 M phosphate-buffered saline (PBS) for choroid isolation. To isolate the choroid, the retina and RPE were removed as a sheet with a small spatula. Occasionally, small bits of RPE would adhere to the choroid, and these were removed by gentle brushing with a sable brush and rinsing with PBS. After the removal of all visible pigment, the choroids were separated from the sclera with a fine spatula and snap frozen in microfuge tubes in liquid nitrogen.

Reverse Transcription–Quantitative PCR (RT-qPCR)

Isolated choroids were pooled separately from control and treated eyes after 0 and 1 day of recovery (three groups of six control and six treated eyes each) and were snap frozen in liquid nitrogen. Additionally, choroids were isolated from individual pairs of control and treated eyes after 0 hour, 6 hours, 12 hours, 1 day, 4 days, 8 days, and 15 days of recovery and were snap frozen in liquid nitrogen. Total RNA was isolated from each group of choroids or individual choroids using an RNA/DNA/protein extraction reagent (Trizol; Invitrogen, Carlsbad, CA) and a cleanup kit (RNeasy MinElute CleanUp; Qiagen, Valencia, CA). RNA was frozen in liquid nitrogen and stored at −80°C until use. RNA concentration and purity were determined at an optical density ratio of 260/280 using a spectrophotometer (ND-1000; NanoDrop Technologies, Wilmington, DE). cDNA was generated from total RNA (14–113 ng) by reverse transcription with MuLV reverse transcriptase and random hexamers according to the manufacturer's protocol (GeneAmp RNA PCR Kit; Applied Biosystems, Foster City, CA). RT-qPCR was performed in triplicate using gene-specific chicken primers together with nucleic acid stain (SYBR Green; Molecular Probes, Eugene, OR) in a 96-well plate format and a PCR detection system (i-Cycler iQTM Multi-Color Real-Time PCR Detection System; Bio-Rad, Hercules, CA). PCR was carried out in a total reaction volume of 25 μL/well. The PCR protocol consisted of an initial denaturation step at 95°C for 90 seconds, followed by 40 cycles of amplification at 95°C for 45 seconds, 60°C for 45 seconds, and 72°C for 60 seconds. Samples were again denaturated at 95°C for 2 minutes. Melt curve analysis was carried out after PCR amplification by slowly heating samples from 60° to 95°C (70 cycles, increasing temperature 0.5° every 2 minutes). Samples were then maintained on a hold cycle at 15°C until they were collected. During heating, emission of nucleic acid stain (SYBR Green; Molecular Probes) was continuously monitored at 490 nm.

Primers were selected from chick sequences of HAS2 and glyceraldehyde 3-phosphate dehydrogenase (GAPDH) using BLAST, Primer3 (http://frodo.wi.mit.edu/cgi-bin/primer3/primer3_www.cgi) and σ-Genosys (St. Louis, MO; Table 1). The HAS2 PCR product was cloned into the PBluescript SK+ vector (Stratagene, La Jolla, CA) according to the manufacturer's protocol, and its sequence was confirmed by DNA sequencing using a capillary DNA sequencer (ABI 3730; Applied Biosystems, Foster City, CA). GAPDH primers were designed to span three introns yielding a 740-bp product if genomic DNA contamination of cDNA was present. The chicken GAPDH gene was also used as a reference gene to normalize for variation in starting cDNA between samples. Relative levels of gene expression were determined using the mean normalized expression (MNE) values, as previously described.[26,27] Correct product size, lack of primer-dimer formation, and lack of genomic DNA contamination were confirmed by DNA agarose-gel electrophoresis and melt curve analysis, respectively. As an addi-

Table 1. RT-qPCR Gene Primers

Gene Name	Forward Primer	Reverse Primer	Primer Efficiency (%)	Product Size (bp)
HAS2	5′-GGAATCACCGCTGCTTACAT-3′	5′-TGAGTTCCCATCAATGACCA-3′	101.3	300
GAPDH	5′-TGCTAAGGCTGTGGGGAAAGTC-3′	5′-CAAAGGTGGAGGAATGGCTGTC-3′	108.6	248

tional control for genomic DNA contamination, reverse transcriptase was omitted from some choroid RNA samples before reverse transcription.

Quantification of GAPDH transcript copy numbers was achieved by comparison with a standard curve constructed using 10-fold dilutions of the purified 248-bp GAPDH PCR product (3.74×10^2 to 3.74×10^{10} copies of GAPDH) using the same RT-qPCR protocol described here. All samples were amplified in triplicate. Standard curves were obtained by plotting the log of the copy number against the threshold cycle number. Linear regression analysis of the data generated an equation used to estimate the number of copies of GAPDH.

HA Tissue Distribution

The distribution of HA in control and recovering chicken choroids was determined by histochemical staining with a biotinylated HA binding protein (b-HABP; Associates of Cape Cod Inc., East Falmouth, MA) from the HA-binding region of aggrecan, which binds strongly and specifically to HA in cells and tissue sections.[28–31] Punches (5 mm) containing retina, RPE choroid, and sclera were obtained from the posterior poles of control and recovering chick eyes, fixed in neutral-buffered formalin, and embedded in paraffin, and sections were obtained. Tissue sections of posterior ocular tissues were deparaffinized through a graded series of xylenes and ethanol and preincubated with Hanks' balanced salt solution (HBSS) containing 2% fetal bovine serum (FBS; 30 minutes at 22°). Tissue sections were incubated with a solution (5 μg/mL) containing b-HABP in HBSS containing 2% FBS for approximately 16 hours to overnight at 4°C. The slides were washed three times with HBSS/2% FBS and then were incubated with a solution containing fluorescein-streptavidin (Invitrogen) (1:500) in HBSS/2% FBS for 1 hour at 22°C. Sections were rinsed in HBSS/2% FBS, and coverslips were mounted onto the slides with reagent containing 4', 6-diamidino-2-phenylindole (DAPI) (Prolong Gold Antifade; Invitrogen). The labeled sections were viewed by confocal microscopy, using a laser-scanning confocal microscope (Fluoview 1000; Olympus, Center Valley, PA). Specific controls were made by digesting tissue-HA with 100 TRU/mL *Streptomyces hyalurolyticus* hyaluronidase (Sigma-Aldrich, St. Louis, MO) at 60°C in 0.1 M phosphate buffer, pH 7, for 2 hours[32] before labeling with HABP or by adding soluble hyaluronan to the HABP (1/1 wt/wt) for 16 hours at 4°C before incubation on the tissue sections.

HA Quantification by SEC-MALLS

Analyses of HA concentration, size distribution, and weight-average molar mass (M_w) in isolated choroids were conducted by size exclusion chromatography-multiangle laser light scattering (SEC-MALLS), as previously described.[33] Choroids were isolated from recovering and control eyes, pooled separately in groups of three or four, and incubated overnight at 60°C in 0.5 mL of 0.1 M sodium phosphate, pH 6.5, 10 mM EDTA with 0.05% (wt/vol) proteinase K (protease type XXVIII; Sigma-Aldrich,). Pooling of samples was necessary to provide enough material to run two to three replicates per sample and a hyaluronidase control for choroid samples from untreated eyes (with low HA) and treated samples (with high HA). Digests were heated in a 100°C water bath for 10 minutes and centrifuged at 20,000*g* for 20 minutes at 4°C, and the supernatants were removed and extracted once with 3 vol chloroform/methanol (3:1). The top aqueous layer was removed and centrifuged under vacuum for 15 minutes at 22°C to remove residual solvents, and sample volumes were brought to 500 μL with PBS. SEC-MALLS analyses were performed using size exclusion columns (PL Aquagel-OH 60 and PL Aquagel-OH 40; Polymer Laboratories), in series, at 22°C with a flow rate of 0.5 mL/min in 50 mM sodium phosphate, pH 7.0, 150 mM NaCl, and 0.05% (wt/vol) sodium azide. MALLS analyses of the SEC column eluate were performed in line using a photometer (Dawn DSP Laser; Wyatt Technologies, Clinton, SC) in series with a refractometer (Optilab DSP Interferometric Refractometer; Wyatt Technologies). Data were analyzed using ASTRA version 4.73, a dn/dc value of 0.153 mL/g, and second-order Berry fits. All HA concentrations and M_w values shown were the average values from at least two SEC-MALLS runs of each sample. To confirm that the SEC-MALLS signals detected were caused by HA, a portion of each sample was treated with 6 U *S. hyalurolyticus* hyaluronidase (Sigma-Aldrich) in 50 mM $NaPO_4$, pH 7.0, and 150 mM NaCl at 37°C for 24 hours.

Statistical Analysis

Linear regression analyses was performed on RT-qPCR data (Prism version 4.03 for Windows; GraphPad Software, San Diego, CA). Comparisons of gene expression between treated and contralateral control eyes were made using Student's *t*-test for matched pairs or the Wilcoxon matched pairs signed rank test (Prism version 4.03 for Windows; GraphPad Software). Comparisons between groups were made with one-way ANOVA using Scheffé's comparisons and Bonferroni adjustments for multiple comparisons (GB Stat; Dynamic Microsystems, Inc., Silver Spring, MD).

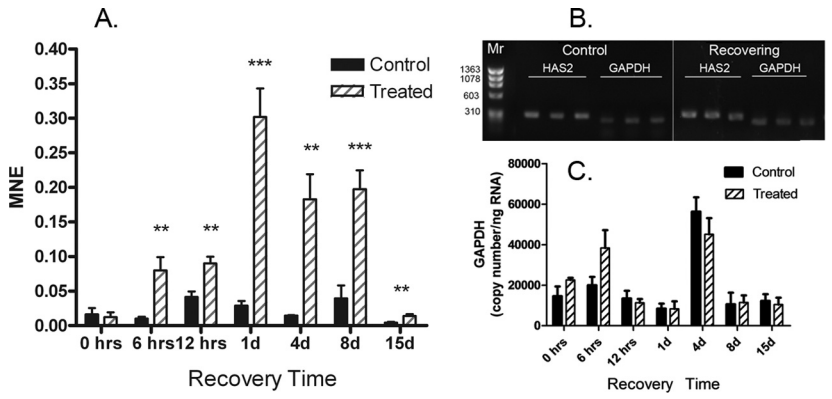

Figure 1. Real-time PCR quantification of *HAS2* gene expression in control and treated eyes. (**A**) Relative HAS2 mRNA abundance was compared in control and treated chick eyes after 10 days of form deprivation (0) and 1 to 15 days of unrestricted vision preceded by 10 days of form deprivation (recovery). Graphs represent the MNE calculated for HAS2 and normalized to the reference gene, *GAPDH*. (**B**) DNA gel electrophoresis of RT-qPCR products for HAS2 and GAPDH. (**C**) Estimated GAPDH copy number per nanogram of total RNA in control and treated eyes. All reactions were run in triplicate and repeated on two or three separate RT-qPCR procedures. $^{**}P < 0.01$, $^{***}P < 0.001$, Student's paired *t*-test; $n = 4$–5 birds in each group.

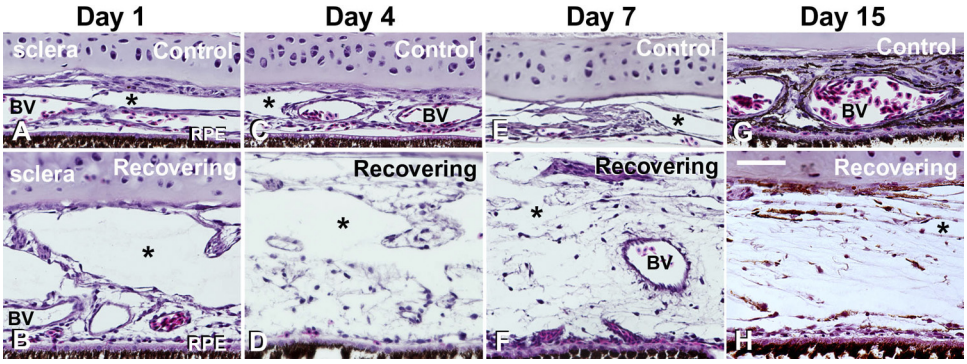

FIGURE 2. Light micrographs of transverse sections through the sclera-choroid-RPE of control and treated chicken eyes after 1, 4, 7, and 15 days of recovery from form-deprivation myopia. Note the expansion of the choroid and the appearance of thin-walled lymphatic channels on the scleral side of the choroid (*asterisks*). Erythrocytes can be seen in large and small blood vessels (BV). Scale bar, 50 μm.

RESULTS

Choroidal Expression of HAS2

Because of the significant upregulation of HAS2 in chick choroids after 1 day of recovery and the known role of HA in the extracellular matrix during tissue growth and differentiation, HAS2 expression was compared in the choroids of control and treated eyes after 0 hour, 6 hours, 12 hours, 1 day, 4 days, 8 days, and 15 days of recovery by RT-qPCR (Fig. 1A). Expression levels of HAS2 were calculated in control and recovering chick choroids with the cycle threshold values normalized to the reference gene *GAPDH* using MNE. After 10 days of visual deprivation, no significant differences were detected in HAS2 expression in choroids of treated eyes compared with controls ($P = 0.765$, paired *t*-test). Interestingly, HAS2 expression was significantly higher in treated eyes after only 6 hours of unrestricted vision compared with contralateral controls (average MNE = 0.080 ± 0.019 compared with 0.010 ± 0.003; $n = 10$; $P < 0.01$, paired *t*-test). HAS2 expression remained significantly elevated in treated eyes for 8 days of recovery. After 15 days of recovery, HAS2 mRNA expression decreased to levels significantly below those observed in treated eyes after 1 day, 4 days, or 8 days of recovery ($P < 0.05$; ANOVA with Scheffé comparison and Bonferroni correction). However, HAS2 mRNA levels were still significantly higher in treated eyes than in paired controls after 15 days of recovery ($P < 0.01$, paired *t*-test). No significant differences were detected in HAS2 mRNA relative expression levels among any of the seven control groups (0 hour to day 15) ($P > 0.05$; Scheffé comparison and Bonferroni correction). All RT-qPCR products were analyzed by ethidium bromide gel electrophoresis to verify the correct size and amplification of HAS2 (300 bp) and GAPDH (248 bp) in chick choroids (Fig. 1B). No PCR products were detected when reverse transcriptase was omitted from the reverse transcription reaction.

The expression of GAPDH was quantified in choroid RNA samples from contralateral control and treated eyes using a standard curve generated by RT-qPCR (Fig. 1C). A linear relationship between log copy number of GAPDH and the threshold cycle was established (slope = −3.197; *Y*-intercept = 41.34; $r^2 = 0.9659$) (data not shown). No significant differences were detected in GAPDH expression between contralateral control and treated eyes throughout the treatment period (paired *t*-test), although both control and treated choroids at the 4-day time point had significantly higher GAPDH copies than all other groups with the exception of the 6-hour recovering group ($P < 0.05$; Scheffé comparison and Bonferroni correction). In a previous study,[34] microarray analysis indicated that GAPDH expression was significantly lower in retina/choroid/RPE preparations of eyes recovering from induced myopia for 1 day compared with contralateral control eyes. In these preparations, the retina contributed the most RNA to the RNA preparations because the retina has the greatest cell density of the three. We suspect that the decreased GAPDH expression observed in the previous study reflected a general downregulation of cellular activity in the retina (perhaps induced by the previous form deprivation) because the retina was the most cellular tissue and, therefore, contributed the most RNA to the pooled tissue samples. No amplification of HAS2 or GAPDH occurred in the absence of reverse transcriptase during reverse transcription.

HA Changes in Chick Choroid

Choroid morphology over the 15-day recovery period was assessed on tissue sections of the posterior poles of control and recovering chick eyes (Figs. 2A–H). Control choroids varied

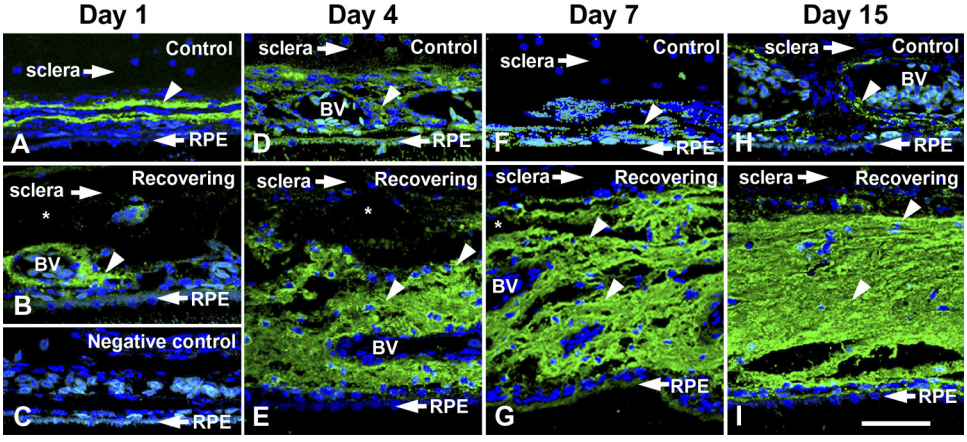

FIGURE 3. HA staining in control (*top*) and recovering (*bottom*) chick choroids. Choroids were stained for HA using b-HABP (HA binding region of aggrecan protein) followed by incubation in fluorescein-streptavidin. After 4 days of recovery and throughout the treatment period, there is more intense HA (*green*) staining in recovering choroids (**E**, **G**, **I**) compared with contralateral controls (*arrowheads*; **D**, **F**, **H**). HA accumulates in the choroidal stroma between blood vessels (BV) and lymphatic channels (*asterisks*). Negative control of a control choroid in which the biotinylated-HABP was omitted in the incubation procedure (**C**). *Blue*: DAPI staining of the nuclei. Scale bar, 50 μm.

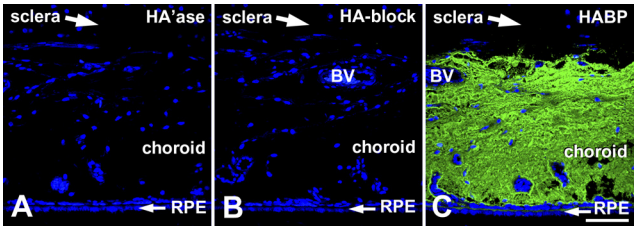

FIGURE 4. Specificity of HA staining in choroids from recovering eyes. (**A**) Predigestion of tissue sections (from a day 15 recovering eye) with *S. hyalurolyticus* hyaluronidase (100 U/mL) before labeling with b-HABP and fluorescein-streptavidin resulted in complete suppression of HA labeling. (**B**) Preincubation of b-HABP with HA before use on tissue sections also abolished HA labeling. (**C**) Tissue section processed together with those used in Figures 5A and 5B from the posterior ocular wall of a chick eye after recovery for 15 days and labeled with b-HABP and fluorescein-streptavidin shows intense HA labeling throughout the choroidal stroma. Nuclei were stained with DAPI. Scale bar, 50 μm.

somewhat in thickness within the same tissue section; however, there was not a general trend to see thicker choroids with increasing age. After 1 day of recovery, choroids of treated eyes appeared thicker than those of control eyes, largely because of the expansion of large lymphatic lacunae in the suprachoroidal space (asterisk). Additionally, after 4 days of recovery, the extravascular choroidal stroma appeared expanded and edematous and remained so throughout the 15-day recovery period.

HA was detected in tissue sections using a biotinylated fragment of aggrecan containing the specific and high-affinity HA binding region (b-HABP; Figs. 3A–I). HA was closely associated with perivascular sheaths of larger choroidal blood vessels in control eyes (arrowheads, Figs. 3A, 3D, 3F, 3H) and in eyes after 1 day of recovery (arrowhead, Fig. 4B). After 4, 7, and 15 days of recovery, increasing levels of HA were apparent throughout the choroidal stroma and appeared to occupy the majority of the extravascular space extending from the RPE to the choroid-sclera junction. This HA accumulation appeared to displace the choroidal stromal cells (most apparent in the 7-day and 15-day treated eyes), resulting in a lower cell density in the expanding choroids. The specificity of b-HABP staining for HA in tissue sections was verified with two types of controls. One negative control consisted of a tissue section (from a 15-day recovering eye) that was incubated with *S. hyalurolyticus* hyaluronidase, an enzyme specific for HA before labeling with b-HABP and fluorescein-streptavidin (Fig. 4A). The second control was the blocking of b-HABP by the addition of HA (1:1 HA/b-HABP) to b-HABP before use on a tissue section (Fig. 4B). For comparison, an additional section from the same 15-day recovering eye was labeled with b-HABR, followed by fluorescein-streptavidin, and was processed together with the negative controls (Fig. 4C). HA labeling was completely abolished when sections were digested with hyaluronidase or when b-HABP binding was blocked with HA.

Chick Choroid HA Content and Size

To obtain quantitative data about HA changes, the size distribution, M_w value, and concentration of HA in choroids of treated and control eyes were assessed using SEC-MALLS (Fig. 5A). SEC-MALLS is one of the best methods to assess HA molar mass and size distributions and to determine HA concentration. HA was readily detected in choroids of recovering eyes (4–20 days), whereas HA was low or undetectable in control samples. Digestion of choroid samples with *S. hyalurolyticus* hyaluronidase before SEC-MALLS analyses indicated that 91% ± 5% of the total refractive index peaks were HA (Fig. 5B). MALLS analyses indicated that the molar mass distributions of HA

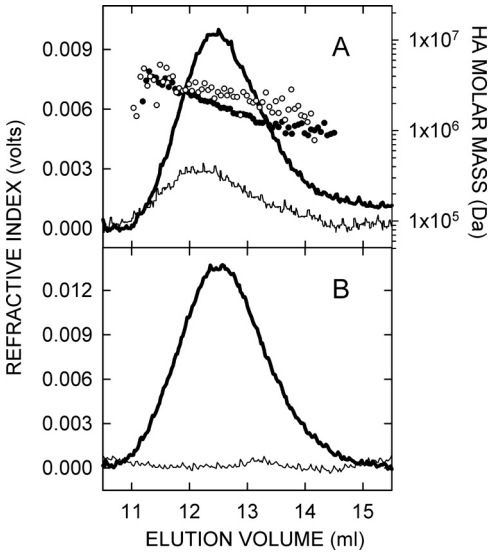

FIGURE 5. SEC-MALLS analyses of choroidal HA. (**A**) Chromatograms from SEC-MALLS of choroid samples from day 8 recovering and contralateral control chick eyes. *Lines*: refractive index traces indicating the amount of HA. *Individual points*: M_w values calculated from the laser light scattering data for each time (eluate) interval. Each sample represents four choroids pooled separately from control (*thin line*, *open circles*) and recovering eyes (*thick line*, *solid circles*). (**B**) To confirm that the SEC-MALLS signals detected were caused by HA, a portion of each sample was treated at 37°C for 24 hours with 6 U of *S. hyalurolyticus* hyaluronidase, which specifically digests only HA. Refractive index (concentration) traces are shown for a choroid sample from a day 7 recovering eye that was untreated (*thick line*) or hyaluronidase-treated (*thin line*). Signal reduction in this digested sample was 96%. Overall, the HA content of samples was at least 91% ± 5% (n = 28).

chains ranged from 1 MDa to 4 MDa in all choroid samples. The M_w values of HA calculated for pooled choroid samples from control or treated eyes ranged from 1.96 MDa to 2.36 MDa, with no significant changes in HA size distribution between control and treated choroids throughout the treatment period (Fig. 6).

HA content in posterior chick choroids was also determined by SEC-MALLS analyses in two or three separate pools of

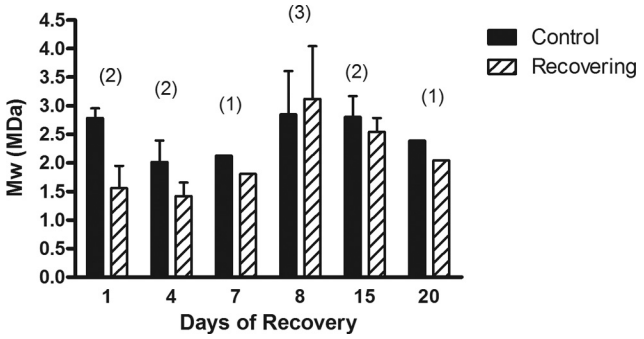

FIGURE 6. SEC-MALLS analysis of HA size in control and treated choroids. HA mass was calculated from pooled choroid samples (n = 3–4 choroids/pool) from control (*solid bars*) and treated/recovering (*diagonal bars*) eyes analyzed as in Figure 5. Data are expressed as the molecular mass (M_w) in megadaltons (MDa) in pooled choroid samples (n = 3–4) obtained after 1, 4, 8, 15, and 20 days of recovery. Values are the means of three independent MALLS experiments. *Bars*: standard error (for day 8 sample) or range of two independent experiments (for days 1, 4, 15). Data for days 7 and 20 represent one experiment. Numbers in parentheses indicate the sample sizes for each group of pooled samples.

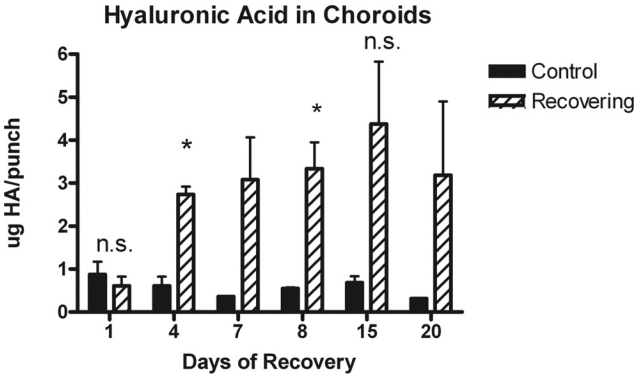

FIGURE 7. Quantification of HA in choroid samples from recovering and contralateral control chick eyes using SEC-MALLS. Amounts of HA in choroid samples were determined from refractive index traces (as in Fig. 5) as integrated areas under the predominant HA peak. Data are expressed as micrograms HA/choroid punch after 1, 4, 8, 15, and 20 days of recovery. Each choroid sample represented a pool of three or four control or treated choroids. Values are the means of at least three independent MALLS experiments. *Bars*: standard error (days 1, 4, 8, 15) or the range of two independent experiments (days 7, 20). $^*P < 0.05$; n.s., not significant.

choroidal punches isolated from control and recovering eyes (3–4 choroids per pool; Fig. 7). After 4 days of recovery, HA was elevated in recovering choroids compared with contralateral controls (≈3.5-fold) and remained elevated throughout the treatment period (≈5- to 9-fold), although greater variability was noted in samples isolated after 15 and 20 days of recovery. Paired Student's *t*-tests were used to compare HA concentrations in choroids of control and treated eyes. HA levels were significantly elevated in treated choroids after 4 and 8 days of recovery ($P < 0.05$; $n = 3$ separate pools of control and treated choroids), whereas no significant differences were detected between control and treated eyes after 1 day or 15 days of recovery. Statistical analyses were not carried out on samples from day 7 or day 20 recovering eyes because of smaller sample sizes ($n = 2$) for these independent experiments.

DISCUSSION

In this study, we determined that HAS2 mRNA pools were significantly increased in the chick choroid within 6 hours of recovery, peaked at 24 hours, and returned to day 0 levels after 15 days of recovery. Although HAS2 mRNA pools in recovering choroids were significantly reduced after 15 days compared with HAS2 mRNA in eyes treated for 6 hours to 8 days, HAS2 mRNA levels in recovering eyes remained significantly elevated compared with 15 day paired controls (≈2-fold), perhaps because of a coincident reduction in *HAS2* gene expression by paired contralateral controls.

HAS2 is 1 of 3 isoenzymes (HAS1, HAS2, and HAS3) that synthesize HA at the plasma membrane. Each isozyme is the product of a separate gene,[23,35] and each produces HA that differs in size distribution and M_w.[36,37] Of the three HAS isoenzymes, HAS2 has the lowest basal level of constitutive activity,[38] suggesting that HAS2 is the isoenzyme that most likely modulates HA synthesis rates. In a variety of normal and disease conditions, increases in steady state HAS2 mRNA levels are correlated with increased HA biosynthesis,[39–42] although HA product size is variable. Within the eye, expression of one or more HAS isoenzymes has been detected in the retina, choroid, trabecular meshwork cells, corneal endothelial cells, and corneal stromal keratocytes,[39,43–45] where they are predicted to play roles in tissue expansion and growth during normal developmental processes and in proliferative and fibrotic disease processes.

The significant elevation of HAS2 mRNA after only 6 hours of recovery suggests that HA plays a role in the rapid expansion of the choroid that occurs in response to myopic defocus, which was induced in this study by visual form deprivation for 10 days followed by varying periods of unrestricted vision. Therefore, the amount and distribution of HA was evaluated on tissue sections of choroids of control eyes and in choroids after 1 to 15 days of unrestricted vision (recovery). HA was demonstrated in association with the perivascular sheaths of choroidal blood vessels of control eyes and treated eyes after 1 day of recovery. With longer periods of recovery, HA also accumulated in the extravascular stroma of the expanding choroids, occupying the vast majority of space between the RPE and the sclera.

This increased accumulation of HA in recovering choroids was confirmed by MALLS analyses, which indicated that HA content was significantly elevated in choroids from 4 to 8 days of recovery compared with controls. HA concentrations were highly variable in choroids from eyes allowed to recover for 15 and 20 days, although the average levels were 5- to 9-fold higher in experimental eyes compared with controls, respectively. We speculate that HA remains in the expanded choroids of recovering eyes and may be cleared from the stroma as myopic defocus is reduced, resulting in choroidal thinning. However, under our experimental conditions, recovering choroids remained expanded for up to 50 days of recovery, undergoing only a slight thinning after 30 days of recovery.[18]

Interestingly, results from this study indicate that HAS2 mRNA pools were reduced to levels comparable to control levels after 15 days of recovery. These data suggest that increased HA synthesis by HAS2 early in the recovery process results in increased accumulation of HA in the choroidal stroma for up to 8 days, at which time synthesis rates drop and choroidal HA concentrations may gradually decrease as the choroid thins. Depending on the tissue, the metabolic half-life, or clearance rate, of HA can be minutes (e.g., blood), less than a day (e.g., skin), or weeks to months (e.g., cartilage).[46]

In mammals, HA turns over and is removed from extracellular matrices in tissues through local degradation or drainage into the lymphatic system for clearance and catabolism in regional lymph nodes and liver.[46–48] This systemic and continuous HA turnover process is mediated by the HA receptor for endocytosis[49,50] (Stabilin-2), a scavenger receptor that also mediates the clearance of chondroitin sulfates and heparin.[51,52] There does not appear to be a Stabilin-2 gene homologue in the *Gallus gallus* genome, and the chick receptor that removes HA and other GAGs from the circulation has not yet been identified. HA catabolism is regulated through the action of one or more hyaluronidases (hyaluronoglucosaminidases). In the chicken, at least three putative hyaluronidases have been identified: HYAL1, HYAL2, and HYAL4 (http://www.ncbi.nlm.nih.gov, provided in the public domain by the National Center for Biotechnology Information, Bethesda, MD). We speculate that changes in choroidal synthesis of one or more of these hyaluronidases, in addition to changes in HAS2 expression or activity, play a role in the turnover of HA from the choroid, as has been demonstrated in the developing cornea[53] limb,[54] and, more recently, the retina.[55] In these systems, and likely as well as in the chick myopic defocus response reported here, early rapid accumulation of HA is needed for subsequent cellular infiltration and extracellular matrix remodeling, during which the accumulated HA is usually removed. The well-developed lymphatic channels present in the suprachoroidal space of the chick choroid may be involved in the removal of HA from the choroidal stroma, by diffusion or hydrodynamic forces, and delivery to a systemic clearance system for degradation. Inter-

estingly, in mammals HA in the eye is ultimately degraded in the liver.[48]

MALLS analyses indicated that choroidal HA has a calculated M_w of approximately 2 MDa in control and recovering eyes. HA is a heterogeneous polymer ranging in size from 5000 Da to 10,000,000 Da (25,000 disaccharides) in vivo. In many cases, the cellular response to HA depends on the molecular mass of the polymer chains. Lower molecular mass HA (<500 kDa) has been shown to participate in receptor-mediated activation of transcription factors that are involved in angiogenesis,[56] malignancy,[57] and inflammatory responses,[58] whereas higher molecular mass HA (>1000 kDa) is an extracellular and pericellular matrix component that contributes to structural integrity, tissue hydration, lubrication, and biomechanics.[59] High molecular mass HA has also been shown to regulate cell adhesion, migration, and differentiation.[60,61] MALLS analyses indicated that approximately 90% of choroidal HA is high molecular mass (1–4 MDa), consistent with the HA product sizes known to be synthesized by HAS2. We therefore conclude that newly synthesized HA becomes hydrated, expands the choroidal stroma, and is largely responsible for the stromal swelling observed during the recovery from myopia.

The rapid upregulation of HAS2 mRNA suggests that the *HAS2* gene is a primary target in the choroid for retinal/retinal pigment epithelial transcription factors produced in response to myopic defocus. The *HAS2* gene has been demonstrated to be a primary epidermal growth factor and retinoic acid responding gene, containing two retinoic acid response elements and STAT-response elements in the promoter.[40] Additionally, HAS2 has been demonstrated to be rapidly (within 2 hours) upregulated by TGF-β in cultures of corneal keratocytes,[39] corneal endothelial cells,[62] and trabecular meshwork cells.[45] Both retinoic acid and TGF-β have been implicated in the retina-choroid-sclera cascade. Retinoic acid synthesis has been shown to increase significantly in isolated chick choroids, after 6 hours of recovery from diffuser wear, and continues to increase for at least the first 24 hours of recovery.[63] Based on the similar temporal changes observed for choroidal retinoic acid synthesis and HAS2 mRNA pools, it is possible that retinoic acid may regulate choroidal expression of the *HAS2* gene. Further studies are necessary to establish a causal role between choroidal retinoic acid synthesis and choroidal *HAS2* gene expression. Studies evaluating TGF-β in a variety of ocular tissues during visually induced changes in ocular growth have been inconclusive, with some reporting increased TGF-β2 in both the retina-RPE-choroid and the sclera of myopic chick eyes.[64] Others report decreased TGF-β levels in the retina, RPE, and choroid during the development of myopia in chicks.[65] Decreased RNA levels of the TGF-β isoforms TGF-β1, TGF-β2, and TGF-β3 have also been reported in the tree shrew sclera during myopia development.[66] Further studies are necessary to determine whether TGF-β is involved in the regulation of HAS2 expression in the choroid.

The cells responsible for HA synthesis in the choroid are unknown. HA is known to be synthesized by many cell types, including endothelial cells, fibroblasts, and smooth muscle cells. Based on the uniform distribution of HA within the recovering choroid, we speculate that choroidal stromal fibroblasts or extravascular smooth muscle cells are responsible for the increased HA synthesis associated with choroidal expansion during recovery from induced myopia. Additional experiments are necessary, however, to identify these choroidal cells and the signaling molecules responsible for HAS2 upregulation. Understanding of the molecular regulation of *HAS2* gene expression in the choroid may provide insight into signaling mechanisms underlying visually guided ocular growth regulation and the pathophysiology of several ocular conditions involving choroidal neovascularization, malignancy, and degeneration.

Acknowledgments

The authors thank Randal May and Courtney Houchen (Advanced Immunohistochemistry and Morphology Core, University of Oklahoma Health Science Center) for providing equipment and assistance with light microscopy and Carla Hansen (Department of Cell Biology, University of Oklahoma Health Science Center) for tissue processing, embedding, and sectioning.

References

1. O'Leary DJ, Millodot M. Eyelid closure causes myopia in humans. *Experientia*. 1979;35:1478–1479.
2. Rabin J, Van Sluyters RC, Malach R. Emmetropization: a vision-dependent phenomenon. *Invest Ophthalmol Vis Sci.* 1981;20:561–564.
3. Rasooly R, BenEzra D. Congenital and traumatic cataract: the effect on ocular axial length. *Arch Ophthalmol.* 1988;106:1066–1068.
4. Twomey JM, Gilvarry A, Restori M, Kirkness CM, Moore AT, Holden AL. Ocular enlargement following infantile corneal opacification. *Eye.* 1990;4:497–503.
5. Rada JA, Shelton S, Norton TT. The sclera and myopia. *Exp Eye Res.* 2006;82:185–200.
6. Goss DA, Criswell MH. Myopia development in experimental animals: a literature review. *Am J Optom Physiol Opt.* 1981;58:859–869.
7. Schaeffel F, Glasser A, Howland HC. Accommodation, refractive error and eye growth in chickens. *Vision Res.* 1988;28:639–657.
8. Wallman J, Adams JI. Developmental aspects of experimental myopia in chicks: susceptibility, recovery and relation to emmetropization. *Vision Res.* 1987;27:1139–1163.
9. Winawer J, Wallman J. In a matter of minutes, the eye can know which way to grow. *Invest Ophthalmol Vis Sci.* 2005;46:2238–2241.
10. Wildsoet CF, Schmid KL. Optical correction of form deprivation myopia inhibits refractive recovery in chick eyes with intact or sectioned optic nerves. *Vision Res.* 2000;40:3273–3282.
11. Troilo D, Gottlieb MD, Wallman J. Visual deprivation causes myopia in chicks with optic nerve section. *Curr Eye Res.* 1987;6:993–999.
12. De Stefano ME, Mugnaini E. Fine structure of the choroidal coat of the avian eye: lymphatic vessels. *Invest Ophthalmol Vis Sci.* 1997;38:1241–1260.
13. De Stefano ME, Mugnaini E. Fine structure of the choroidal coat of the avian eye: vascularization, supporting tissue and innervation. *Anat Embryol.* 1997;195:393–418.
14. Junghans BM, Crewther SG, Liang H, Crewther DP, Wareing L, Pirie B. Lymphatics in the chick choroid? *Aust N Z J Ophthalmol.* 1996;24:47–49.
15. Junghans BM, Crewther SG, Liang H, Crewther DP. A role for choroidal lymphatics during recovery from form deprivation myopia. *Optom Vis Sci.* 1999;76:796–803.
16. Wallman J, Wildsoet C, Xu A, et al. Moving the retina: choroidal modulation of refractive state. *Vision Res.* 1995;35:37–50.
17. Liang H, Crewther SG, Crewther DP, Pirie B. Morphology of the recovery from form deprivation myopia in the chick. *Aust N Z J Ophthalmol.* 1996;24:41–44.
18. Rada JA, Huang Y, Rada KG. Identification of choroidal ovotransferrin as a potential ocular growth regulator. *Curr Eye Res.* 2001;22:121–132.
19. Rada JA, McFarland AL, Cornuet PK, Hassell JR. Proteoglycan synthesis by scleral chondrocytes is modulated by a vision dependent mechanism. *Curr Eye Res.* 1992;11:767–782.
20. Hung LF, Wallman J, Smith EL 3rd. Vision-dependent changes in the choroidal thickness of macaque monkeys. *Invest Ophthalmol Vis Sci.* 2000;41:1259–1269.
21. Siegwart JT Jr, Norton TT. The susceptible period for deprivation-induced myopia in tree shrew. *Vision Res.* 1998;38:3505–3515.

22. Troilo D, Nickla DL, Wildsoet CF. Choroidal thickness changes during altered eye growth and refractive state in a primate. *Invest Ophthalmol Vis Sci.* 2000;41:1249–1258.
23. Weigel PH, DeAngelis PL. Hyaluronan synthases: a decade-plus of novel glycosyltransferases. *J Biol Chem.* 2007;282:36777–36781.
24. Weigel PH, Hascall VC, Tammi M. Hyaluronan synthases. *J Biol Chem.* 1997;272:13997–14000.
25. Rada JA, Thoft RA, Hassell JR. Increased aggrecan (cartilage proteoglycan) production in the sclera of myopic chicks. *Dev Biol.* 1991;147:303–312.
26. Shelton LS, Rada JS. Effects of cyclic mechanical stretch on extracellular matrix synthesis by human scleral fibroblasts. *Exp Eye Res.* 2007;84:314–322.
27. Simon P. Q-Gene: processing quantitative real-time RT-PCR data. *Bioinformatics.* 2003;19:1439–1440.
28. Knudson CB, Toole BP. Fluorescent morphological probe for hyaluronate. *J Cell Biol.* 1985;100:1753–1758.
29. Underhill CB, Zhang L. Analysis of hyaluronan using biotinylated hyaluronan-binding proteins. *Methods Mol Biol.* 2000;137:441–447.
30. Shibata S, Fukada K, Imai H, Abe T, Yamashita Y. In situ hybridization and immunohistochemistry of versican, aggrecan and link protein, and histochemistry of hyaluronan in the developing mouse limb bud cartilage. *J Anat.* 2003;203:425–432.
31. Toole BP, Yu Q, Underhill CB. Hyaluronan and hyaluronan-binding proteins: probes for specific detection. *Methods Mol Biol.* 2001; 171:479–485.
32. Yamada K. Effects of novel (streptomyces) hyaluronidase digestion upon some mucosaccharide stainings of the cartilages and aortas in the rabbit and rat. *Histochemie.* 1971;27:277–289.
33. Baggenstoss BA, Weigel PH. Size exclusion chromatography-multiangle laser light scattering analysis of hyaluronan size distributions made by membrane-bound hyaluronan synthase. *Anal Biochem.* 2006;352:243–251.
34. Rada JA, Wiechmann AF. Ocular expression of avian thymic hormone: changes during the recovery from induced myopia. *Mol Vis.* 2009;15:778–792.
35. Itano N, Sawai T, Yoshida M, et al. Three isoforms of mammalian hyaluronan synthases have distinct enzymatic properties. *J Biol Chem.* 1999;274:25085–25092.
36. Brinck J, Heldin P. Expression of recombinant hyaluronan synthase (HAS) isoforms in CHO cells reduces cell migration and cell surface CD44. *Exp Cell Res.* 1999;252:342–351.
37. Köprunner M, Müllegger J, Lepperdinger G. Synthesis of hyaluronan of distinctly different chain length is regulated by differential expression of Xhas1 and 2 during early development of *Xenopus laevis*. *Mech Dev.* 2000;90:275–278.
38. Monslow J, Williams JD, Guy CA, et al. Identification and analysis of the promoter region of the human hyaluronan synthase 2 gene. *J Biol Chem.* 2004;279:20576–20581.
39. Guo N, Kanter D, Funderburgh ML, Mann MM, Du Y, Funderburgh JL. A rapid transient increase in hyaluronan synthase-2 mRNA initiates secretion of hyaluronan by corneal keratocytes in response to transforming growth factor beta. *J Biol Chem.* 2007;282: 12475–12483.
40. Saavalainen K, Pasonen-Seppänen S, Dunlop TW, Tammi R, Tammi MI, Carlberg C. The human hyaluronan synthase 2 gene is a primary retinoic acid and epidermal growth factor responding gene. *J Biol Chem.* 2005;280:14636–14644.
41. Udabage L, Brownlee GR, Nilsson SK, Brown TJ. The over-expression of HAS2, Hyal-2 and CD44 is implicated in the invasiveness of breast cancer. *Exp Cell Res.* 2005;310:205–217.
42. Bakkers J, Kramer C, Pothof J, Quaedvlieg NE, Spaink HP, Hammerschmidt M. Has2 is required upstream of Rac1 to govern dorsal migration of lateral cells during zebrafish gastrulation. *Development.* 2004;131:525–537.
43. Murata M, Horiuchi S. Hyaluronan synthases, hyaluronan and its CD44 receptors in the posterior segment of rabbit eye. *Ophthalmologica.* 2005;219:287–291.
44. Usui T, Amano S, Oshika T, et al. Expression regulation of hyaluronan synthase in corneal endothelial cells. *Invest Ophthalmol Vis Sci.* 2000;41:3261–3267.
45. Usui T, Nakajima F, Ideta R, Kaji, et al. Hyaluronan synthase in trabecular meshwork cells. *Br J Ophthalmol.* 2003;87:357–360.
46. Itano N. Simple primary structure, complex turnover regulation and multiple roles of hyaluronan. *J Biochem.* 2008;144:131–137.
47. Weigel PH, Yik JHN. Glycans as endocytosis signals: the cases of the asialoglycoprotein and hyaluronan/chondroitin sulfate receptors. *Biochim Biophys Acta.* 2002;1572:341–363.
48. Laurent TC, Fraser JRE. Hyaluronan. *FASEB J.* 1992;6:2397–2404.
49. Weigel JA, Raymond RC, McGary CT, Singh A, Weigel PH. A blocking antibody to the hyaluronan (HA) receptor for endocytosis (HARE) inhibits HA clearance by perfused liver. *J Biol Chem.* 2003;278:9802–9812.
50. Zhou B, Weigel JA, Fauss L, Weigel PH. Identification of the hyaluronan receptor for endocytosis (HARE). *J Biol Chem.* 2000; 275:37733–37741.
51. Harris EN, Weigel JA, Weigel PH. Endocytic function, glycosaminoglycan specificity, and antibody sensitivity of the recombinant human 190-kDa HARE. *J Biol Chem.* 2004;279:36201–36209.
52. Harris EN, Weigel JA, Weigel PH. The human hyaluronan receptor for endocytosis (HARE) is a systemic clearance receptor for heparin. *J Biol Chem.* 2008;283:17341–17350.
53. Toole BP, Trelstad RL. Hyaluronate production and removal during corneal development in the chick. *Dev Biol.* 1971;26:28–35.
54. Li Y, Toole BP, Dealy CN, Kosher RA. Hyaluronan in limb morphogenesis. *Dev Biol.* 2007;305:411–420.
55. Inoue Y, Yoneda M, Miyaishi O, Iwaki M, Zako M. Hyaluronan dynamics during retinal development. *Brain Res.* 2009;1256: 55–60.
56. West DC, Hampson IN, Arnold F, Kumar S. Angiogenesis induced by degradation products of hyaluronan. *Science.* 1985;228:1324–1326.
57. Toole BP, Slomiany MG. Hyaluronan: a constitutive regulator of chemoresistance and malignancy in cancer cells. *Semin Cancer Biol.* 2008;18:244–250.
58. Noble PW. Hyaluronan and its catabolic products in tissue injury and repair. *Matrix Biol.* 2002;21:25–29.
59. Almond A. Hyaluronan. *Cell Mol Life Sci.* 2007;64:1591–1596.
60. Toole BP. Hyaluronan: from extracellular glue to pericellular cue. *Nat Rev Cancer.* 2004;4:528–539.
61. Girish KS, Kemparaju K. The magic glue hyaluronan and its eraser hyaluronidase: a biological overview. *Life Sci.* 2007;80:1921–1943.
62. Suzuki K, Yamamoto T, Usui T, Suzuki K, Heldin P, Yamashita H. Expression of hyaluronan synthase in intraocular proliferative diseases: regulation of expression in human vascular endothelial cells by transforming growth factor-beta. *Jpn J Ophthalmol.* 2003; 47:557–564.
63. Mertz JR, Wallman J. Choroidal retinoic acid synthesis: a possible mediator between refractive error and compensatory eye growth. *Exp Eye Res.* 2000;70:519–527.
64. Seko Y, Shimokawa H, Tokoro T. Expression of bFGF and TGF-beta 2 in experimental myopia in chicks. *Invest Ophthalmol Vis Sci.* 1995;36:1183–1187.
65. Honda S, Fujii S, Sekiya Y, et al. Retinal control on the axial length mediated by transforming growth factor-beta in chick eye. *Invest Ophthalmol Vis Sci.* 1996;37:2519–2526.
66. Jobling AI, Nguyen M, Gentle A, et al. Isoform-specific changes in scleral transforming growth factor-beta expression and the regulation of collagen synthesis during myopia progression. *J Biol Chem.* 2004;279:18121–126.